Structural and Spectroscopic Properties of AlN Layers Grown by MOVPE

S.B. Thapa [a,*], C. Kirchner [a], F. Scholz [a], G.M. Prinz [b], K. Thonke [b], R. Sauer [b],
A. Chuvilin [c], J. Biskupek [c], U. Kaiser [c], D. Hofstetter [d]

[a] *Optoelectronics Dept., Ulm University, 89081 Ulm, Germany*
[b] *Semiconductor Physics Dept., Ulm University, 89081 Ulm, Germany*
[c] *Electron Microscopy Group of Materials Science, Ulm University, 89081 Ulm, Germany*
[d] *Optoelectronics Group, University of Neuchatel, CH-2000 Neuchatel, Switzerland*

Abstract

The effects on surface morphology, crystal quality, and growth rate of undoped AlN layers grown on c-plane sapphire substrates due to the changes in growth parameters, such as V-III ratio, N_2-H_2 ratio, and growth temperature in LP-MOVPE are studied here. The optimized growth process resulted in an almost flat surface morphology with a significantly reduced number of hexagonal pits ($3 \cdot 10^7\, cm^{-2}$) and good crystalline quality having a rms value of roughness of 0.4 nm measured by atomic force microscopy and a high resolution x-ray diffraction (HRXRD) FWHM value for (0002) reflection of 200 arcsecs. The threading dislocation density of the AlN layer is estimated approx. $10^9\, cm^{-2}$ from cross-sectional transmission electron microscopy (TEM) measurements. Additionally, these optimized samples show a strong donor-bound exciton luminescence signal with a FWHM of 20 meV. Furthermore, small period AlN/GaN superlattice structures with excellent uniformity were grown, as proven by our HRXRD and TEM studies.

Key words: AlN, MOVPE, Surface morphology, HRXRD, Superlattice
PACS: 81.05.Ea, 81.15.Gh, 78.55.-m, 61.10 Nz, 79.60.Jv

1. Introduction

Due to its wide direct band gap of approx. 6 eV and the associated outstanding chemical and thermal stability, the realization of high-quality AlN epitaxial layers can widely extend the application field of III-V nitride materials versus high–temperature high–power applications, e.g. high–power field effect transistors, and opto-electronic devices, particularly UV diodes, [1–3]. Furthermore, AlN/GaN superlattice structures can be used in optical devices operating at telecommunication wavelengths by exploiting intersubband transitions between bound quantum well states [4,5].

However, the growth of AlN having excellent crystalline quality, smooth surface morphology, and good electrical and optical properties - as required for device fabrication - is still a big challenge. In recent years, various growth techniques have been reported by several groups [?,6–10]. Nonetheless, still lot of ambiguities are prevailing in the relation between basic epitaxial parameters, the respective growth kinetics and resulting crystal quality of AlN layers. In this article, we report the effects of the variation of basic growth parameters in low-pressure metalorganic vapor phase epitaxy (LP-MOVPE) on the surface morphology, crystal quality, growth rate and consequently on the luminescence spectra of the

---

* Corresponding author. Tel.: +49-731-50-26195; Fax: +49-731-50-26049; *E-mail address:* `sarad.thapa@uni-ulm.de` (S.B. Thapa)

AlN layers. After optimizing the AlN growth process, AlN/GaN superlattice structures were grown.

2. Experimental

Undoped layers of AlN, approximately 500 nm thick, were grown on c-plane sapphire substrates in an AIXTRON AIX 200 RF LP-MOVPE system by using TMAl and NH_3 as precursors and H_2 as a carrier gas in N_2 and H_2 gas atmosphere. The growth conditions of the AlN bulk layers were varied with respect to the N_2-H_2 gas composition, V-III ratio, and the growth temperature while keeping the growth pressure constant at 35 mbar, the lower limit of our system. The low temperature AlN nucleation layer was also optimized with respect to the above mentioned growth parameters to obtain good quality of AlN bulk layer.

The surface morphology was analyzed by using atomic force microscopy (AFM) and scanning electron microscopy (SEM). High-resolution X-ray diffraction (HRXRD) rocking curve measurements (with open detector) for the (0002) reflection were carried out to examine the crystal quality of bulk AlN epitaxial layers. Low-temperature (8 K) cathodoluminescence (CL) provided information about the spectroscopic properties. Cross-sectional transmission electron microscopy (TEM) investigations were carried out to observe the defects on the sample.

Meanwhile, AlN/GaN (4 nm / 4 nm) superlattice structures (21 periods) were grown on 500 nm thick $Al_{0.5}Ga_{0.5}N$ buffer layers and capped with 40 nm thick $Al_{0.5}Ga_{0.5}N$. The HRXRD measurement of the ω-2θ scan (0002 reflection) was performed to verify the periodicity and transmission electron microscopy (TEM) was used to examine the abruptness of the interfaces of the superlattice structure.

3. Results and Discussion

At the early stage of this study, our AlN layers exhibited either random 3D nucleated growth features of rough grains or columnar textures. Moreover, hexagonal pits of varying size, depth and diameter (fig. 1, left) are largely observed. In the initial stage of the AlN layer growth, the rearrangement of the atoms may form the columns. The high pit density on the surface is due to such columns protruding through the entire layer as shown in the fig. 2 (top). Similarly, the crystalline quality (as measured

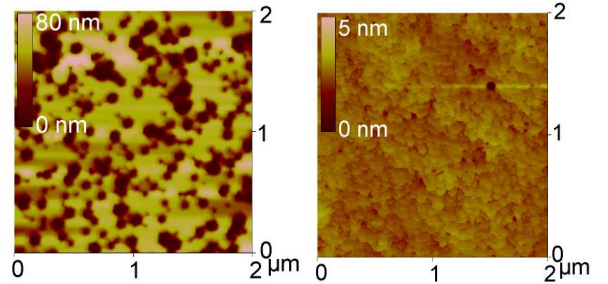by the FWHM of HRXRD) of the layers was much inferior.

Fig. 1. AFM image of bulk AlN layer before (left) and after (right) optimization.

When increasing the growth temperature from $1110°$ to $1170°$, substantial improvements of the surface quality of the bulk AlN layers were observed. AFM measurements have exhibited a remarkable reduction of the rms value of the surface roughness from 21.5 nm to 1.5 nm, and a decrease of the hexagonal pit density approx. from $4 \cdot 10^{10} \, cm^{-2}$ to $7 \cdot 10^7 \, cm^{-2}$. However, a further increase of the growth temperature is restricted by system limitations. Surface transport plays an important role in determining the physical structure. Obviously, the elevated temperature enhances the lateral movement of deposited species resulting in a quasi 2D growth of AlN layers and eventually reducing the pits [11].

One major problem in AlN growth is the parasitic reactions between NH_3 and TMAl in the gas phase, which can be minimized by reducing the reactor pressure, upstream positioning of the substrate on the susceptor [12], and low flow rates of both precursors during growth [13]. Indeed, the FWHM value of the HRXRD (0002) reflection decreases when lowering the V-III ratio. Thus, a low V-III ratio with low flow rates of both precursors is an eminent growth condition for crystallographic perfection. However, at a very low V-III ratio (<500), we observed a degradation of the surface quality with the occasional presence of cracks. Furthermore, an increased growth rate at very low V-III ratio may lead to 3D growth of the AlN which gives rise to inhomogeneous lattice relaxation and generates threading dislocations [14].

It was observed the growth rate decreases with the increase of N_2-H_2 ratio (fig. 3, left) while keeping the total flow constant. This may be caused by the lower diffusivity of the metalorganics in N_2 than in H_2 thus decreasing the transport of group III species
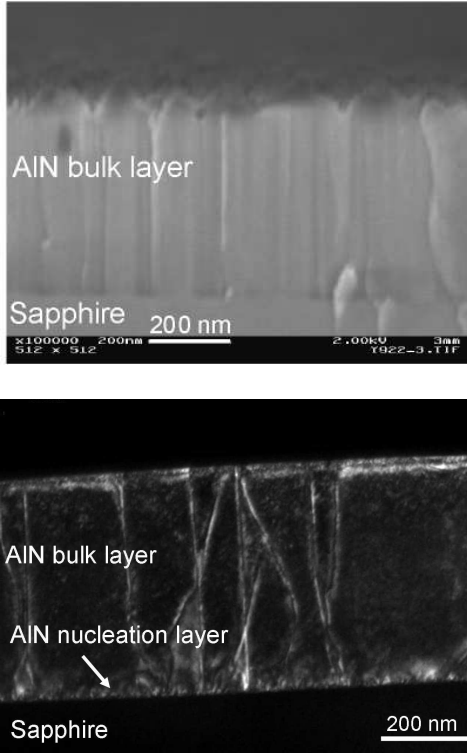
Fig. 2. SEM image of a bulk AlN layer before optimization (top). Weak-beam dark-field TEM image after optimization (below).
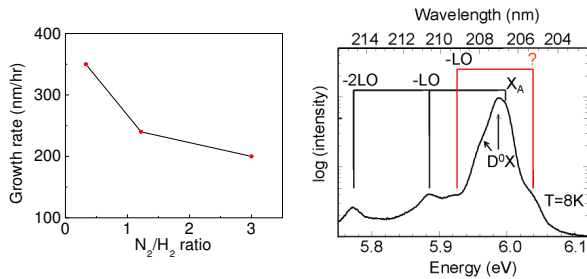

Fig. 3. Change in growth rate with respect to the N_2-H_2 ratio (left). Low-temperature CL spectra of a bulk AlN layer (right).

to the substrate. Moreover, the increased amount of N_2 decreases the substrate temperature [15] which also may explain the decreasing growth rate. This result is somewhat contrary to the observations made by other groups [16] in the high-temperature GaN growth.

With all the above observations, the growth process was finally optimized by decreasing the NH_3 and TMAl flow rates to 250 sccm and 9 μmol/min,

respectively, and thus apparently lowering the V-III ratio to 1200 at a higher growth temperature of $1150°$. The flow rate of N_2 and H_2 was kept at 3:1 and the total flow in the reactor was kept constant at 1700 sccm. Such optimized growth parameters led to an almost flat surface morphology with a significantly reduced hexagonal-shaped pit density of approx. $3 \cdot 10^7 \, cm^{-2}$ and good crystalline quality. Figure 1 (right) shows well ordered atomic steps on the surface of monocrystalline AlN with only few hexagonal pits. We measured a strongly decreased rms roughness of only 0.4 nm and an HRXRD FWHM for (0002) reflection of 200 arcsec. In such layers, a threading dislocation density of approx. $10^9 \, cm^{-2}$ from cross-sectional TEM images using the weak-beam dark-field technique (fig. 2, bottom) can be deduced. Only half of the dislocations thread through the entire layer. The final growth rate of AlN layer was 235 nm/hr.

The excellent crystalline quality is further confirmed by the observation of a strong near band edge emission at ≈ 6 eV, as shown in fig. 3 (right). A line-shape fit of the main peak reveals three lines, which could be assigned to excitons bound to different neutral donors (D^0X, lower in energy) and an a free exciton (X_A) recombination at 6 eV with a FWHM of ≈ 20 meV. This assignment was confirmed by reflection and temperature dependent CL measurements. For layers grown at lower growth rates the intensity of the near band edge luminescence increases. The intensity ratio of the X_A versus that of the D^0X suggests that the overall dopant concentration content is low.

After having obtained the desired crystalline quality and surface morphology of bulk AlN layers, AlN/GaN superlattice structures (SLS) were grown on c-plane sapphire. Figure 4 (top) shows the superlattice related satellite peaks (SL) in HRXRD confirming the good periodicity of the layers. The TEM cross section studies confirm the excellent uniformity and the flatness of the SLS structure. These excellent data have also been confirmed by SIMS. By analyzing TEM-bright-field image (fig. 4, bottom right), we found that the interfaces of AlN on GaN are sharper than those of GaN on AlN. Moreover, as shown in TEM-dark-field image (fig. 4, bottom left) many of the threading dislocations coming through the $Al_{0.5}Ga_{0.5}N$ buffer layer are slightly bent at the interface between the buffer layer and SLS which formed dislocation loops in SLS to annihilate the threading dislocations.
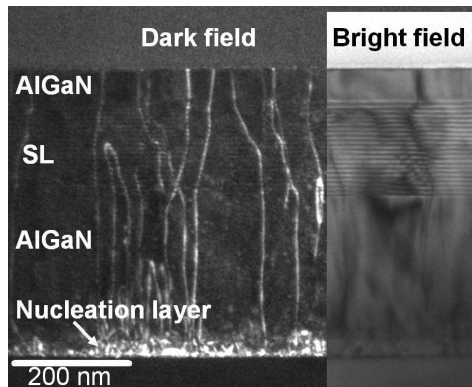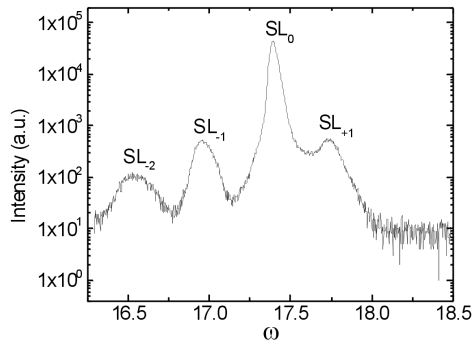
Fig. 4. HRXRD measurement of the ω-2θ scan (0002 reflection) of AlN/GaN superlattice (top). Dark and Bright-field TEM image of the superlattice structure. The brighter contrast within the superlattice corresponds to AlN-layers, the darker one to GaN-layers. Dislocation loops are visible in SLS.

4. Summary

Undoped AlN layers with high crystalline quality and almost flat surface morphology were grown on c-plane sapphires substrate by LP-MOVPE. After optimization, we achieved an rms value of the surface roughness of 0.4 nm, and a HRXRD FWHM for the (0002) reflection of 200 arcsec. The hexagonal pit density is reduced to $3 \cdot 10^7 \, cm^{-2}$ whereas the threading dislocation density is estimated approx. $10^9 \, cm^{-2}$) from cross-sectional TEM measurement. Low-temperature CL spectra demonstrate the good optical quality of the AlN layers. Consequently, it was possible to grow AlN/GaN superlattice structures having good periodicity and abruptness of the AlN/GaN interfaces.

5. Acknowledgement

References

[1] C.R. Miskys, J.A. Garrido, C.E. Nebel, M. Hermann, O. Ambacher, M. Eickhoff, M. Stutzmann, Appl. Phys. Lett. 82 (2) (2003) 290.

[2] G. Kipshidze, V. Kuryatkov, K. Zhu, B. Borisov, M. Holtz, S. Nikishin, H. Temkin, J. Appl. Phys. 93 (3) (2003) 1363.

[3] Y. Taniyashu M. Kasu T. Makimoto, Appl. Phys. Lett. 84 (12) (2004) 2115.

[4] D. Hofstetter, S. Schad, H. Wu, W.J. Schaff, L.F. Eastman Appl. Phys. Lett. 83 (3) (2002) 572.

[5] I. Waki, C. Kumtornkittikul, Y. Shimogaki, Y. Nakano, Appl. Phys. Lett. 82 (25) (2002) 4465.

[6] F. Yan, M. Tsukihara, A. Nakamura, T. Yadani, T. Fukumoto, Y. Naoi, S. Sakai, Jpn. J. Appl. Phys. 43 (8B) (2004) L1057.

[7] Q. Paduano, D. Weyburne, Jpn. J. Appl. Phys. 44 (4) (2005) L150.

[8] C. McAleese, M.J. Kappers, R.A. Oliver, R. Datta, E.J. Thrush, C.J. Humphreys, proc. Int. 11th European Workshop on MOVPE, Lausanne, June 5th–8th 2005.

[9] K. Kawaguchi, A. Kuramata, Jpn. J. Appl. Phys. 44 (46) (2005) L1400.

[10] J. Bai, M. Dudley, W.H. Sun, H.M. Wang, M.Asif Khan, Appl. Phys. Lett. 88 (2006) 051903.

[11] A. Nakajima, Y. Furukawa, S. Koga, H. Yonezu, J. Cryst. Growth 265 (2004) 351.

[12] C. Kirchner, P. Brückner, F. Scholz, G. Prinz, K. Thonke, D. Hofstetter, proc. Int. 11th European Workshop on MOVPE, Lausanne, June 5th–8th 2005.

[13] A.V. Lobanova, K.M. Mazaev, R.A. Talalaev, M. Leys, S. Boeykens, J. Cryst. Growth 287 (2006) 601.

[14] A. Nakajima, Y. Furukawa, H. Yokoya, S. Yamaguchi, H. Yonezu, Jpn. J. Appl. Phys. 45 (4A) (2006) 2422.

[15] N. Kaluza, R. Steins, Y.S. Cho, Z. Sofer, and H. Hardtdegen, proc. Int. 11th European Workshop on MOVPE, Lausanne, June 5th–8th 2005

[16] R. Steins, H. Hardtdegen, N. Kaluja, M.v.d. Ahe, Y.S. Cho, and Z. Sofer, proc. Int. 11th European Workshop on MOVPE, Lausanne, June 5th–8th 2005